Original Article
J. Korean Wood Sci. Technol. 2024, 52(3): 221-233
https://doi.org/10.5658/WOOD.2024.52.3.221

Journal of the Korean Wood Science and Technology
pISSN: 1017-0715 eISSN: 2233-7180
http://www.woodj.org

Effect of Ethanol Fractionation of Lignin on the Physicochemical Properties of Lignin-Based Polyurethane Film

Sungwook WON[1] · Junsik BANG[1] · Sang-Woo PARK[1] · Jungkyu KIM[1] · Minjung JUNG[1] · Seungoh JUNG[1] · Heecheol YUN[1] · Hwanmyeong YEO[1,2] · In-Gyu CHOI[1,2] · Hyo Won KWAK[1,2,†]

ABSTRACT

Lignin, a prominent constituent of woody biomass, is abundant in nature, cost-effective, and contains various functional groups, including hydroxyl groups. Owing to these characteristics, they have the potential to replace petroleum-based polyols in the polyurethane industry, offering a solution to environmental problems linked to resource depletion and CO_2 emissions. However, the structural complexity and low reactivity of lignin present challenges for its direct application in polyurethane materials. In this study, Kraft lignin (KL), a representative technical lignin, was fractionated with ethanol, an eco-friendly solvent, and mixed with conventional polyols in varying proportions to produce polyurethane films. The results of ethanol fractionation showed that the polydispersity of ethanol-soluble lignin (ESL) decreased from 3.71 to 2.72 and the hydroxyl content of ESL increased from 4.20 mmol/g to 5.49 mmol/g. Consequently, the polyurethane prepared by adding ESL was superior to the KL-based film, exhibiting improved miscibility with petrochemical-based polyols and reactivity with isocyanate groups. Consequently, the films using ESL as the polyol exhibited reduced shrinkage and a more uniform structure. Optical microscope and scanning electron microscope observations confirmed that lignin aggregation was lower in polyurethane with ESL than in that with KL. When the hydrophobicity of the samples was measured using the water contact angle, the addition of ESL resulted in higher hydrophobicity. In addition, as the amount of ESL added increased, an increase of 7.4% in the residual char was observed, and a 4.04% increase in T_{max} the thermal stability of the produced polyurethane was effectively improved.

Keywords: lignin, ethanol, fractionation, thermal stability, polyurethane

1. INTRODUCTION

Polyurethane (PU) is the general term used for all substances with urethane bonds formed by the reaction of polyols with two or more hydroxyl groups and two or more isocyanate groups. The mechanical properties, such as hardness and flexibility, can be adjusted by varying the ratio of the polyol and isocyanate groups. In

Date Received December 29, 2023; Date Revised January 16, 2024; Date Accepted February 19, 2024; Published May 25, 2024
[1] Department of Agriculture, Forestry and Bioresources, College of Agriculture & Life Sciences, Seoul National University, Seoul 08826, Korea
[2] Research Institute of Agriculture and Life Sciences, Seoul National University, Seoul 08826, Korea
[†] Corresponding author: Hyo Won KWAK (e-mail: bk0502@snu.ac.kr, https://orcid.org/0000-0003-1630-7210)

addition, owing to its excellent durability, toughness, and chemical resistance, it is used in various industrial fields such as coatings, adhesives, foams, films, textiles, and medical care (Das and Mahanwar, 2020; Kim *et al*., 2002; Lee and Oh, 2023; Li *et al*., 2017). However, both polyols and isocyanates, the main raw materials of PU, are manufactured in the petrochemical industry and use large amounts of energy in the production process, which leads to environmental pollution issues such as carbon dioxide emissions and resource depletion. Therefore, there has been growing interest in the need for a variety of environmentally friendly materials to replace petrochemical-based materials (Akindoyo *et al*., 2016).

Lignin is the second most abundant natural biomass polymer on Earth and is a major by-product of the chemical treatment of wood fibers in the pulp industry (Bang *et al*., 2022; Hwang *et al*., 2021). It is an amorphous three-dimensional molecule formed by random radical cross-linking polymerization between phenylpropanoid monomers during biosynthesis (Kim *et al*., 2019), with varying compositions of *p*-coumaryl alcohol (H-unit), coniferyl alcohol (G-unit), and synapyl alcohol (S-unit) depending on the plant source (Figueiredo *et al*., 2018; Zendrato *et al*., 2021). Lignin molecules contain a variety of functional groups, including phenolic hydroxyl, carboxyl, methoxy, and aldehyde groups, indicating their potential use as high-value added materials in various industrial fields (Hasan *et al*., 2023; Lee *et al*., 2021a). In particular, they have the potential to replace petrochemical-based polyols owing to their high hydroxyl content. In addition, they have various advantages such as low cost, high thermal stability, biodegradability, UV protection, antioxidation, and thermal stability (Choi *et al*., 2021; Das and Mahanwar, 2020; Kim *et al*., 2023a), etc. However, most lignin is utilized only for energy recovery in the paper industry (Bang *et al*., 2023; Kwak *et al*., 2016), and the technology has not been fully developed because of its low miscibility and reactivity (Park *et al*., 2023). In the biosynthesis of lignin, it has an irregular structure and a wide molecular weight distribution, making it difficult to introduce into raw polymer materials that require chemical reactions. This results in their aggregation and poor miscibility with other substances and solvents (Ajao *et al*., 2019; Jääskeläinen *et al*., 2017). Therefore, to incorporate lignin into the PU industry, it is essential to have a low molecular weight, good polydispersity (PDI), high hydroxyl group content, and high reactivity.

Solvent fractionation is the most efficient method to improve the uniformity of lignin, offering the flexibility to obtain the desired lignin molecular weight based on solvent selection (Kim *et al*., 2017; Lee *et al*., 2021b; Park *et al*., 2018, 2020). Moreover, solvent fractionation is less expensive than other methods and can be easily combined with other processes (Kang *et al*., 2013; Pang *et al*., 2021; Watumlawar and Park, 2023). Solvent fractionation can also increase lignin purity. Because lignin and hemicellulose are strongly bound to each other in the lignin-carbohydrate complex (Fatriasari *et al*., 2020), solvent fractionation can remove hemicellulose, which is strongly bound to some of the lignin (Gigli and Crestini, 2020). Ethanol is a popular solvent for the solvent fractionation of lignin. Because it is a polar protic solvent, it can induce the demethylation of lignin, which is favorable for increasing the hydroxyl content (Ponnuchamy *et al*., 2021). In addition, it is inexpensive and eco-friendly compared with other organic solvents, and its low boiling point makes it more reusable than other solvents (Tekin *et al*., 2018). Therefore, in this study, ethanol was selected as the solvent for lignin fractionation.

In this study, kraft lignin (KL), the most commonly used technical lignin for lignin applications, was used. The lignin was fractionated using ethanol, which is an eco-friendly solvent, so that it could have suitable properties to replace petroleum-based polyols. Additionally, PU films were prepared using KL and ethanol-fractionated lignin as biopolyols with 4,4'-diphenylmethane diiso-

cyanate (MDI), and their physicochemical properties were evaluated.

2. MATRERIALS and METHODS

2.1. Materials

KL was kindly provided by Moorim P&P (Ulsan, Korea). The KL was dried in an oven for 24 h before use. Polyethylene glycol (PEG, M_n = 400) and ethanol (99%) were purchased from SamChun Chemical (Seoul, Korea); MDI (NCO% = 33.6) and Tetrahydrofuran (THF, 99%) were purchased from Daejung Chemicals & Metals (Siheung, Korea); and dibutyltin dilaurate (DBTDL) was purchased from Junsei Chemical (Tokyo, Japan). 2-Chloro-4,4,5,5-tetramethyl-1,3,2-dioxaphospholane (TMDP), pyridine, deuterated chloroform ($CDCl_3$), cyclohexanol, and chromium acetylacetonate were purchased from Sigma Aldrich (Yongin, Korea).

2.2. Ethanol fractionation of kraft lignin

To obtain ethanol-soluble lignin (ESL), dried KL was added to 200 mL ethanol and stirred at room temperature for 24 h (400 rpm). Subsequently, ESL and ethanol-insoluble lignin (EIL) were separated using a vacuum filter with a 3 μm pore size filter paper. The ESL solution was obtained through rotary evaporation, and EIL was dried in a 60℃ oven for 24 hours. The filtered EIL solid was dried in an oven using filter paper. The ESL yield was calculated based on the weights of the dried EIL. The ESL yield was calculated using Equation (1):

$$ESL\ yield\ (\%) = \frac{x_0 - (x_{paper} + x_{EIL})}{x_0} \times 100, \quad (1)$$

Where χ_0 is the weight of the dried KL before fractionation and χ_{paper} is the weight of the filter paper. χ_{EIL} is the weight of the dried EIL sample (Lee *et al*., 2021b; Park *et al*., 2018).

2.3. Preparation of base lignin and fractionated lignin-based polyurethane films

Lignin-based PU films were prepared using a solvent casting method (Wang *et al*., 2019). First, PEG and MDI were added to THF (40 mL) in appropriate ratios, followed by the addition of 5 wt% DBTDL as a catalyst. MDI provides isocyanate groups that react with hydroxyl groups to form urethane bonds. The mixture was stirred at 60℃ for 30 min to prepare a prepolymer (400 rpm). KL and ESL were then added, and the resulting mixture was stirred again at 60℃ for 30 min. The mixed solution was sonicated to remove the residual bubbles. The solution was poured onto a Teflon plate with a diameter of 10 cm, and the solvent was evaporated in a hood for 24 h. The films were then cured at 60℃ in an oven for 48 h. The ratios of the films are listed in Table 1.

2.4. Characterization of kraft lignin, ethanol-soluble lignin and lignin-based polyurethane

The molecular weights of KL, ESL, and EIL were measured by gel permeation chromatography (GPC, LC-40, Shimadzu, Kyoto, Japan) with THF as the solvent. Additionally, the hydroxyl group content of each sample was measured using phosphorous-31 nuclear magnetic resonance (^{31}P NMR; Advance 600 MHz high-resolution spectrometer, Bruker, Ettlingen, Germany). Each lignin sample was dried in an oven for 24 hours, followed by weighting 20–25 mg. Then 400, 150, and 70 μL of solvent solution, mixture solution, and TMDP were added, respectively. The solvent solution was prepared by mixing pyridine and $CDCl_3$ at a 1.6:1 V/V ratio. The mixture was prepared by adding 100 mg of cyclohexanol and 90 mg of chromium acetylacetonate to 25 mL of the prepared solvent solution.

Fourier transform infrared spectroscopy (FT-IR, Sum-

Table 1. Chemical composition of PU samples

Variable	PEG	PEG1/KL1	PEG2/KL1	PEG3/KL1	PEG1/ESL1	PEG2/ESL1	PEG3/ESL1
PEG (wt%)	59.7	30.8	40.6	45.5	29.3	39.4	44.4
KL (wt%)	.	30.8	20.3	15.2	.	.	.
ESL (wt%)	.	.	.	.	29.3	19.6	14.8
MDI (wt%)	37.3	35.4	36.1	36.4	38.5	38.1	37.9
DBTDL (wt%)	5	5	5	5	5	5	5
NCO index	100	118	120	112	118	109	108
NCO/OH ratio	1.0	1.0	1.0	1.0	1.0	1.0	1.0

PU: polyurethane, PEG: polyethylene glycol, KL: kraft lignin, ESL: ethanol-soluble lignin, MDI: 4,4'-diphenylmethane diisocyanate, DBTDL: dibutyltin dilaurate.

mit, Thermo Fisher Scientific, Waltham, MA, USA) in attenuated total reflectance mode was performed to confirm the chemical bonding characteristics of the lignin-based PU. The range scanned was 4,000−525 cm^{-1}, with a scan resolution of 4 cm^{-1}. The surface and cross-section of the lignin-based PU were observed using an optical microscope (OM, ECLIPSE LV100ND, Nikon, Tokyo, Japan) and a field-emission scanning electron microscope (FE-SEM, SUPRA 55VP, Carl Zeiss, Oberkochen, Germany), respectively. The SEM samples were coated using a platinum sputter coater (EM SCD005, Leica, Wetzlar, Germany). The hydrophobicity of the lignin-based PU was analyzed using water contact angle measurements and a swelling ratio evaluation. For water contact angle analysis, ImageJ software (National Institutes of Health, Bethesda, MD, USA) was used. To evaluate the swelling ratio, all samples were dried in a 60℃ oven for 24 hours. The dried samples were cut into 1 cm × 1 cm pieces, placed in 20 mL of distilled water, removed after five days, and weighed after removing any remaining surface moisture. This value was calculated using Equation (2):

$$Swelling\ ratio\ (\%) = \frac{m_s - m_0}{m_0} \times 100, \quad (2)$$

Where m_0 is the weight of the dried sample and m_s is the weight of the swollen sample.

The thermal behavior of KL and ESL and the thermal stability of the lignin-based PU were measured using thermogravimetric analysis (TGA, TA Instruments, New Castle, DE, USA) and derivative thermogravimetry (DTG). The samples were heated from room temperature to 800℃ at a heating rate of 10℃ min^{-1}.

3. RESULTS and DISCUSSION

3.1. Chemical structure analysis of kraft lignin, ethanol-soluble lignin and ethanol-insoluble lignin

After lignin-ethanol fractionation, the mass yield of ESL was 72.4 wt% of the initial KL. These results are similar to those of a previous study (Ponnuchamy *et al*., 2021). Fig. 1(a) shows the FT-IR spectra of lignin obtained after the ethanol fractionation of lignins (ESL and EIL) and the original KL. The broad peaks at 3,500 −3,000 cm^{-1} represent aliphatic and aromatic hydroxyl groups, whereas the peak at 2,940 cm^{-1} represents C-H symmetric vibrations. The peak at 1,700 cm^{-1} is attributed to the stretching of unconjugated carbonyl and conjugated ester bonds from phenolic acids, while the peaks

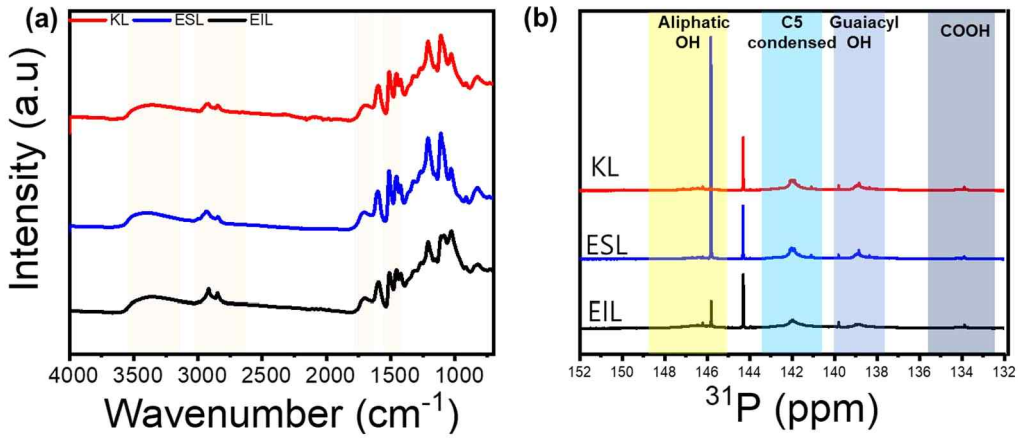

Fig. 1. Characterization of KL, ESL and EIL. (a) FT-IR spectra and (b) ^{31}P-NMR spectra of KL, ESL and EIL. KL: kraft lignin, ESL: ethanol-soluble lignin, EIL: ethanol-insoluble lignin, FT-IR: Fourier transform infrared spectroscopy, ^{31}P-NMR: phosphorous-31 nuclear magnetic resonance.

observed at 1,599, 1,510 and 1,423 cm^{-1} are indicative of the vibrational frequencies of the aromatic backbones. It can be seen that all three types of lignin have a similar chemical structure, and the fractionation did not alter the structure. Fig. 1(b) and Table 2 show the hydroxyl content of each lignin obtained from the ^{31}P-NMR measurements. After ethanol fractionation, the amount of aliphatic OH increased from 0.38 mmol/g to 1.59 mmol/g, while the aromatic hydroxyl content remained almost unchanged. Consequently, the total hydroxyl group content increased more in ESL than in KL. Table 3 shows that M_n, M_w, and PDI all had lower ESL values than KL, decreasing from 840 Da to 490 Da, 3,140 Da to 1,340 Da, and 3.71 to 2.72, respectively. Therefore, ethanol fractionation makes it possible to obtain low-molecular-weight lignin with a high hydroxyl content and improved molecular uniformity.

Table 2. ^{31}P-NMR analysis of KL, ESL and EIL

Variable	KL	ESL	EIL
Aliphatic OH (mmol/g)	0.38	1.59	0.93
COOH (mmol/g)	0.01	0.04	0.02
C5 condensed (mmol/g)	2.65	2.65	2.02
Guaiacyl OH (mmol/g)	1.16	1.12	0.80
Total OH (mmol/g)	4.20	5.49	3.77

^{31}P-NMR: phosphorous-31 nuclear magnetic resonance, KL: kraft lignin, ESL: ethanol-soluble lignin, EIL: ethanol-insoluble lignin.

Table 3. Number-average molecular weight (M_n), weight-average molecular weight (M_w) and polydispersity (PDI) of KL, ESL and EIL determined by GPC

Variable	KL	ESL	EIL
M_n (Da)	840	490	770
M_w (Da)	3,140	1,340	4,970
PDI	3.71	2.72	6.50

KL: kraft lignin, ESL: ethanol-soluble lignin, EIL: ethanol-insoluble lignin, GPC: gel permeation chromatography.

3.2. Thermal properties of lignin and ethanol-fractionated lignin

The thermal properties of KL and ESL were confirmed using TGA, and the results are shown in Fig. 1. Both lignins showed similar thermal properties, with four main types of decomposition. The initial stage, which occurs up to approximately 120℃, is characterized by a loss in weight due to the evaporation of residual moisture. Subsequently, in the temperature range of 120℃ to 400℃, the degradation is marked by the disruption of bonds with relatively low binding energy, encompassing processes such as dehydrogenation, hydroxyl cracking, and the cleavage of ether bonds. Following this, pyrolysis occurs within the temperature range of 400℃ to 600℃, involving the breaking of β-O-4 and α-O-4 linkages, consequently leading to the generation of phenolic compounds. The final stage, observed between 600℃ to 800℃, is defined by the fracture of aromatic rings within the lignin structure. At this stage, decomposition of the functional groups within the lignin molecule was facilitated, leading to the formation of new bonds between the side chains. This process ultimately resulted in the generation of char. The TGA and DTG graphs in Fig. 2 show that the differences in T_{max} and residual char between KL and ESL were not significant. This suggests that ethanol fractionation did not markedly alter thermal characteristics.

3.3. Morphology characterization of lignin and fractionated lignin-based bio-polyurethanes

By manufacturing lignin-based PU via solvent casting (Fig. 3), a film with a more stable structure was obtained when ESL was used than when KL was used. In particular, the KL-added PU film exhibited a wrinkled form and strong shrinkage as the addition ratio of KL increased, whereas such shrinkage and wrinkle formation were not observed in the ESL-applied film. The morphological characteristics of the PU films prepared using the lignin-based biopolyol were analyzed using OM (Fig. 4) and SEM (Fig. 5). Fig. 4 shows the OM image of the lignin-based PU film. In the case of the PU film containing KL, lignin aggregates were observed; as the ratio of KL increased, the size of the aggregates also increased. Meanwhile, in the case of the PU film to which ESL was applied, the formation of aggregates was suppressed, and the size of the produced aggregates was smaller than that of KL. Fig. 5 shows an

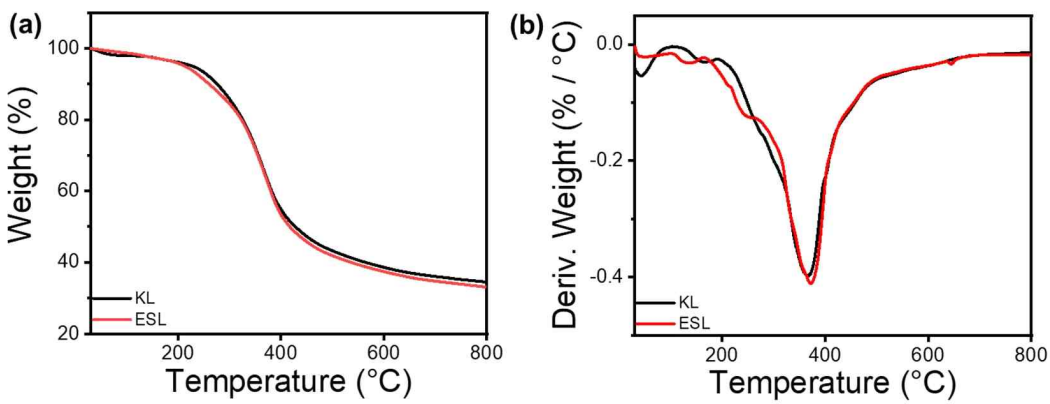

Fig. 2. Thermal properties of KL and ESL. (a) TGA graph and (b) DTG graph of KL and ESL. KL: kraft lignin, ESL: ethanol-soluble lignin, TGA: thermogravimetric analysis, DTG: derivative thermogravimetry.

Fig. 3. Digital images of lignin-based PU films prepared by solvent casting (bar = 500 mm). PEG: polyethylene glycol, KL: kraft lignin, ESL: ethanol-soluble lignin, PU: polyurethane.

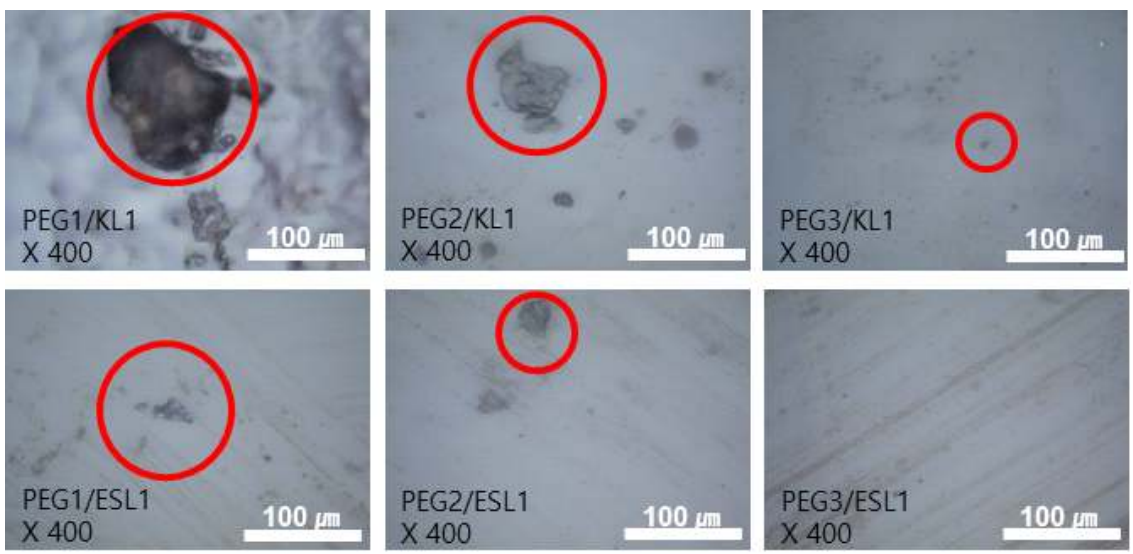

Fig. 4. OM images of lignin-based PU films (bar = 100 μm). PEG: polyethylene glycol, KL: kraft lignin, ESL: ethanol-soluble lignin, OM: optical microscope, PU: polyurethane.

SEM image of the fractured surface of a PU film treated with lignin as a biopolyol. Similar to the OM results, in the case of the PU film containing KL, lignin aggregates were observed on the fracture surface. The aggregation of these lignin molecular structures can be attributed to enhanced intermolecular interactions such as π-π interactions, hydrogen bonds, and dispersion force as the molecular size of lignin increases (Kim *et al*., 2023b). This strong aggregation of the lignin molecules ultimately causes shrinkage of the resulting PU film. In addi-

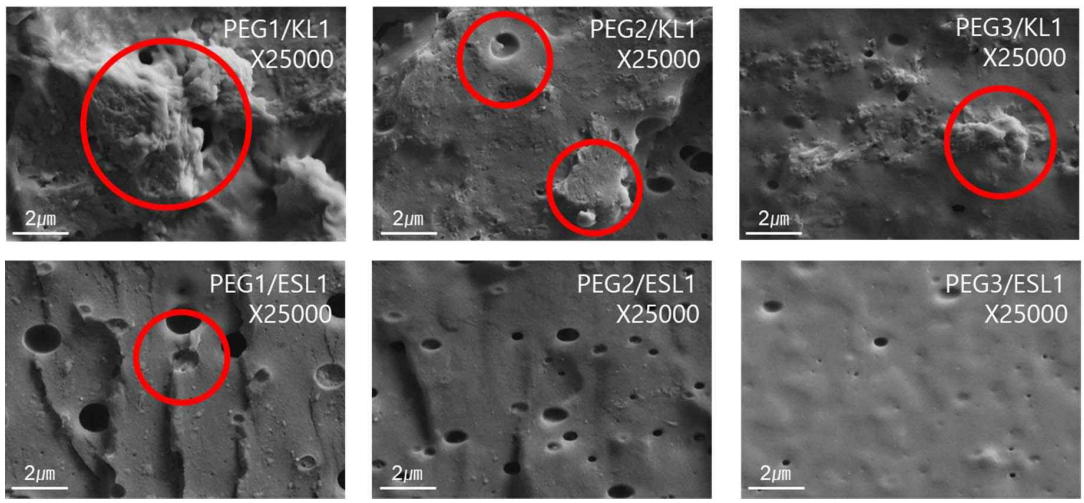

Fig. 5. SEM images of the fracture surfaces of lignin-based PU films (bar = 2 μm). PEG: polyethylene glycol, KL: kraft lignin, ESL: ethanol-soluble lignin, SEM: scanning electron microscope, PU: polyurethane.

tion, the complex structure of the original lignin reduced the extent to which the hydroxyl groups in the molecule reacted with isocyanate. This causes the unreacted lignin to aggregate during polymerization. Meanwhile, in the case of PU with ESL, no aggregates were observed on the fracture surface, and small voids were observed, which is a general phenomenon that occurs in solvent casting. ESL has a higher hydroxyl group content and a less complex structure than KL, allowing it to react well with MDI to form a continuous network and effectively replace PEG, a traditional petrochemical-based polyol (Haridevan *et al*., 2022). In addition, as shown in Table 2, ethanol fractionation resulted in a higher hydroxyl content, which increased the number of active hydroxyl groups and made them more reactive (Ding *et al*., 2018).

3.4. Chemical structure analysis of bio-polyurethane films

The FT-IR spectra of the lignin-based PU films are shown in Fig. 6. As shown in Fig. 4, the FT-IR spectra of lignin-based PU films with different proportions of lignin were similar. First, the disappearance of the peaks around 3,600–3,000 cm^{-1} corresponding to the hydroxyl group and 2,270 cm^{-1} corresponding to the isocyanate group indicates that both functional groups participated in the urethane bonding reaction. As the lignin content increased, the 1,700 cm^{-1} peak corresponding to the carbonyl group (C = O) decreased because the hydroxyl group density and reactivity of aromatic lignin were lower than those of chain-type PEG. Compared to the KL-based film, the carbonyl group (C = O) peak reduction phenomenon of the ESL-based urethane film was relatively weak. This means that as the molecular weight of lignin decreases and the hydroxyl group content per unit mass increases during the ethanol fractionation process, it becomes easier to participate in the urethane bond. The FT-IR results show that ESL has good reactivity and more hydroxyl groups than KL in the PU films, and thus has a high potential to replace conventional petrochemical-based polyols.

3.5. Hydrophobicity of bio-based polyurethane

Lignin is synthesized by random radical polymeriza-

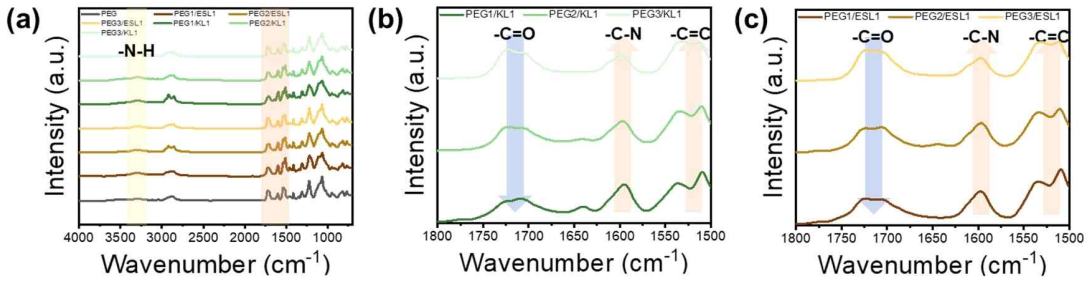

Fig. 6. The FT-IR spectrum of lignin-based PU films. PEG: polyethylene glycol, ESL: ethanol-soluble lignin, KL: kraft lignin, FT-IR: Fourier transform infrared spectroscopy, PU: polyurethane.

tion during biosynthesis, resulting in a complex, three-dimensional heterogeneous structure and an abundance of benzene rings, which form a solid structure that prevents water and insects from entering the wood. Thus, lignin is responsible for the hydrophobicity of wood (Bang *et al*., 2022; Novo-Uzal *et al*., 2012). It is expected that using lignin as a polyol can impart hydrophobicity to PU films. Fig. 7(a–g) show the water contact angles of the PU films prepared with different PEG/lignin ratios. The contact angle of PU with lignin as the biopolyol is larger than that of PU with PEG only. This means that when lignin is introduced into PU films, the hydrophobic properties of lignin are imparted to the films. Also, the contact angle of the PU film using ESL polyol was larger than that of KL. Fig. 7(h) shows the swelling ratios of the PU films. The films with KL showed a larger swelling ratio than the petrochemical-based PU, whereas the films with ESL showed a smaller value. It can also be seen that the contact angle decreased significantly and the swelling ratio increased significantly as the amount of added KL increased. However, the contact angles and swelling ratios did not change significantly with the amount of ESL added to the films. This reason can be interpreted as the miscibility of lignin, and as shown in Figs. 4 and 5, ESL with a small molecular weight and high hydroxyl group content has better miscibility with petrochemical-based polyols, reacts well with isocyanate groups and can better form urethane bonds than KL. Therefore, because the hydrophobicity of the film is caused by lignin, the ESL-based films with well-dispersed lignin exhibited pronounced hydrophobicity.

3.6. Thermal property of bio-based polyurethanes

TGA was performed to evaluate the thermal stability of the PU films using lignin-based polyols. The TGA and DTG results for lignin-based PU are shown in Fig. 6(a) and (b), respectively. The thermal degradation behavior of petroleum-based PU can be divided into three main phases. The initial trace heat loss was attributed to the evaporation of residual solvents and water. The subsequent pyrolysis behavior seen around 250℃ is caused by the degradation of unstable urethane bonds (Wang *et al*., 2013). Finally, it can be seen that the amount of residue above 500℃ rises with increasing lignin addition. The TGA results showed that PEG2/KL1 and PEG2/ESL1, which had relatively low lignin polyol contents, showed initial thermal decomposition behavior similar to that of PU using only PEG polyol, but the residual amount of char was low. This is due to the presence of unstable urethane linkages in lignin-based polyols. Meanwhile, in the case of PEG1/ESL1,

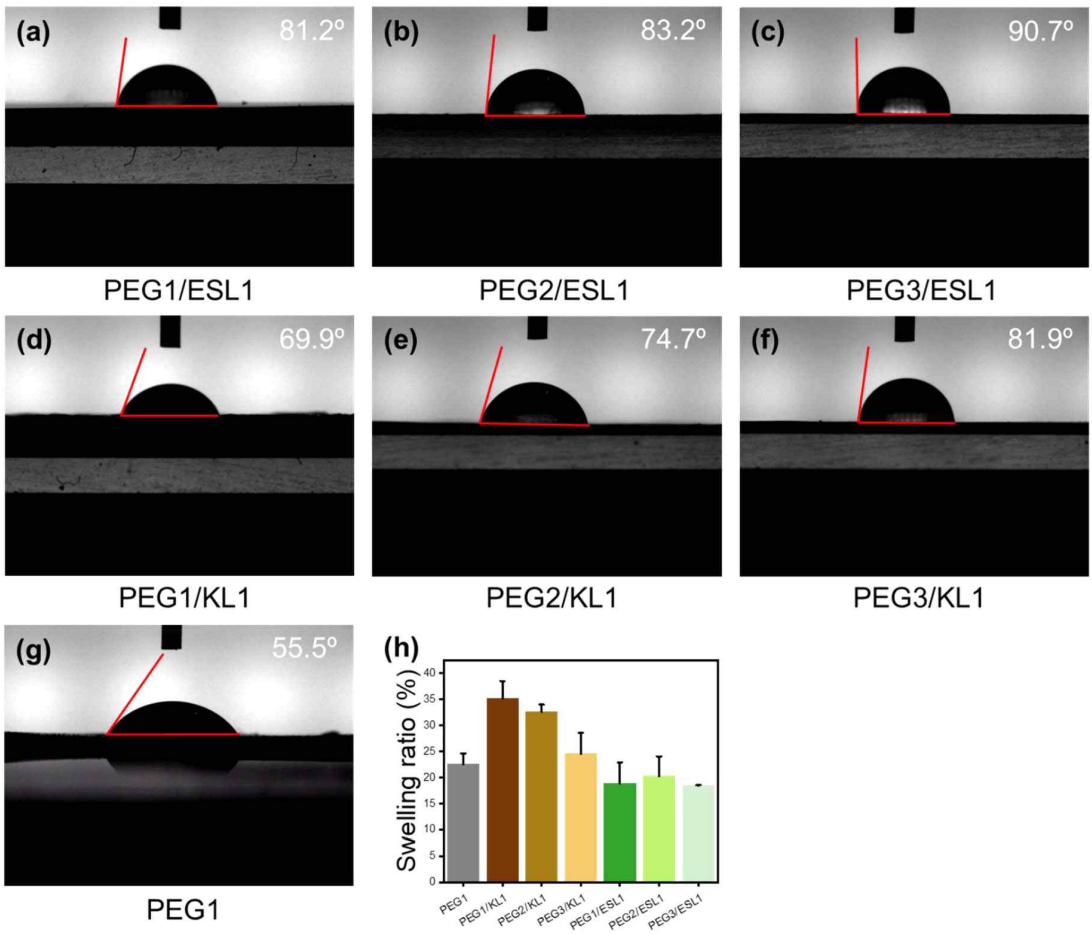

Fig. 7. Hydrophobic properties of lignin-based PU films. (a–g) Water contact angle and (h) swelling ratio of the PU film prepared at different PEG/lignin ratio of polyol. (a) PEG1/KL1, (b) PEG2/KL1, (c) PEG3/KL1, (d) PEG1/ESL1, (e) PEG2/ESL1, (f) PEG3/ESL1, and (g) PEG1. PEG: polyethylene glycol, ESL: ethanol-soluble lignin, KL: kraft lignin, PU: polyurethane.

which had a high lignin content, the residual char amount was 7.4% higher than that of PU using existing PEG. This is because ESL was well incorporated into the PU network structure to stably form urethane bonds, which improved the conversion rate to polyaromatic hydrocarbons (PAH) by adding lignin. This indicates that the thermal properties of the prepared PU can be improved by purifying the lignin and controlling the PEG/lignin polyol content (Fig. 8).

4. CONCLUSIONS

In this study, PU films with KL and ESL were prepared to explore the possibility of utilizing lignin as a replacement for polyols in petrochemically based PU. First, KL and ESL were compared, and the molecular weight of ESL was found to be lower than that of KL, whereas the hydroxyl content of ESL was higher than that of KL, confirming the potential of ESL to replace

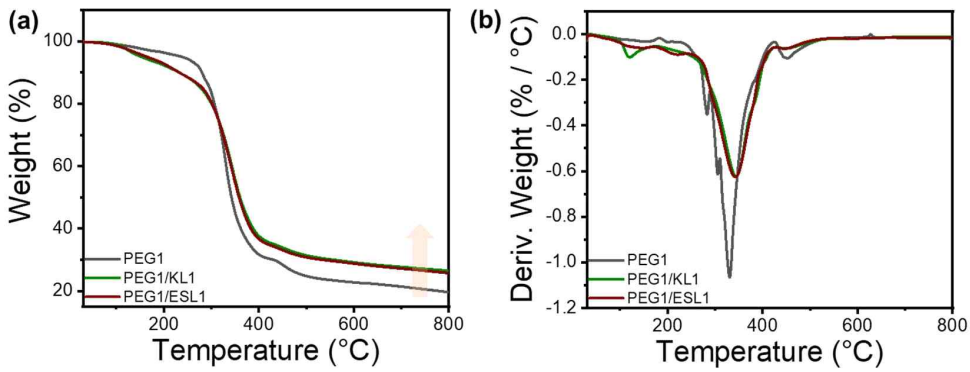

Fig. 8. Thermal properties of lignin-based PU films. (a) TGA graph and (b) DTG graph of lignin-based PU. PEG: polyethylene glycol, KL: kraft lignin, ESL: ethanol-soluble lignin, TGA: thermogravimetric analysis, DTG: derivative thermogravimetry, PU: polyurethane.

petrochemical-based polyols. PU films were prepared with each type of lignin, and the results showed that lignin aggregation was minimized when ESL was added. This is due to the high miscibility of ESL with petrochemical-based PEG polyols and, thus, their improved reactivity with isocyanate groups. It was confirmed that the addition of the ESL increased the contact angle and lowered the swelling ratio, thereby providing hydrophobicity. Finally, the TGA results showed that a large amount of PAH residue was obtained in the ESL-based PU compared to the petrochemical-based PU, indicating that the addition of lignin polyols can impart thermal stability to the prepared PU materials.

CONFLICT of INTEREST

No potential conflict of interest relevant to this article was reported.

ACKNOWLEDGMENT

This study was carried out with the support of the 'R&D Program for Forest Science Technology (2020224 D10-2222-AC02)' provided by the Korea Forest Service (Korea Forestry Promotion Institute). This study was carried out with the support of the 'R&D Program for Forest Science Technology (2020215B10-2222-AC01)' provided by the Korea Forest Service (Korea Forestry Promotion Institute).

REFERENCES

Ajao, O., Jeaidi, J., Benali, M., Abdelaziz, O.Y., Hulteberg, C.P. 2019. Green solvents-based fractionation process for kraft lignin with controlled dispersity and molecular weight. Bioresource Technology 291: 121799.

Akindoyo, J.O., Beg, M.D.H., Ghazali, S., Islam, M.R., Jeyaratnam, N., Yuvaraj, A.R. 2016. Polyurethane types, synthesis and applications: A review. RSC Advances 6(115): 114453-114482.

Bang, J., Kim, J., Kim, Y., Oh, J.K., Yeo, H., Kwak, H.W. 2022. Preparation and characterization of hydrophobic coatings from carnauba wax/lignin blends. Journal of the Korean Wood Science and Technology 50(3): 149-158.

Bang, J., Kim, J.H., Park, S.W., Kim, J., Jung, M., Jung, S., Kim, J.C., Choi, I.G., Kwak, H.W. 2023. Effect of chemically modified lignin addition on the physicochemical properties of PCL nanofibers. International Journal of Biological

Macromolecules 240: 124330.

Choi, J.H., Cho, S.M., Kim, J.C., Park, S.W., Cho, Y.M., Koo, B., Kwak, H.W., Choi, I.G. 2021. Thermal properties of ethanol organosolv lignin depending on its structure. ACS Omega 6(2): 1534-1546.

Das, A., Mahanwar, P. 2020. A brief discussion on advances in polyurethane applications. Advanced Industrial and Engineering Polymer Research 3(3): 93-101.

Ding, Z., Qiu, X., Fang, Z., Yang, D. 2018. Effect of molecular weight on the reactivity and dispersibility of sulfomethylated alkali lignin modified by horseradish peroxidase. ACS Sustainable Chemistry & Engineering 6(11): 14197-14202.

Fatriasari, W., Nurhamzah, F., Raniya, R., Permana Budi Laksana, R., Anita, S.H., Iswanto, A.H., Hermiati, E. 2020. Enzymatic hydrolysis performance of biomass by the addition of a lignin based biosurfactant. Journal of the Korean Wood Science and Technology 48(5): 651-665.

Figueiredo, P., Lintinen, K., Hirvonen, J.T., Kostiainen, M.A., Santos, H.A. 2018. Properties and chemical modifications of lignin: Towards lignin-based nanomaterials for biomedical applications. Progress in Materials Science 93: 233-269.

Gigli, M., Crestini, C. 2020. Fractionation of industrial lignins: Opportunities and challenges. Green Chemistry 22(15): 4722-4746.

Haridevan, H., Evans, D.A.C., Martin, D.J., Annamalai, P.K. 2022. Rational analysis of dispersion and solubility of kraft lignin in polyols for polyurethanes. Industrial Crops and Products 185: 115129.

Hasan, M.S., Sardar, M.R.I., Shafin, A.A., Rahman, M.S., Mahmud, M., Hossen, M.M. 2023. A brief review on applications of lignin. Journal of Chemical Reviews 5(1): 56-82.

Hwang, U.T., Bae, J., Lee, T., Hwang, S.Y., Kim, J.C., Park, J., Choi, I.G., Kwak, H.W., Hwang, S.W., Yeo, H. 2021. Analysis of carbonization behavior of hydrochar produced by hydrothermal carbonization of lignin and development of a prediction model for carbonization degree using near-infrared spectroscopy. Journal of the Korean Wood Science and Technology 49(3): 213-225.

Jääskeläinen, A.S., Liitiä, T., Mikkelson, A., Tamminen, T. 2017. Aqueous organic solvent fractionation as means to improve lignin homogeneity and purity. Industrial Crops and Products 103: 51-58.

Kang, K.K., Kim, S., Kim, I.H., Lee, C., Kim, B.H. 2013. Selective enrichment of symmetric monounsaturated triacylglycerols from palm stearin by double solvent fractionation. LWT-Food Science and Technology 51(1): 242-252.

Kim, J., Bang, J., Park, S., Jung, M., Jung, S., Yun, H., Kim, J.H., Choi, I.G., Kwak, H.W. 2023a. Enhanced barrier properties of biodegradable PBAT/acetylated lignin films. Sustainable Materials and Technologies 37: e00686.

Kim, J., Kim, Y., Jung, S., Yun, H., Yeo, H., Choi, I.G., Kwak, H.W. 2023b. Cationized lignin loaded alginate beads for efficient Cr(VI) removal. Journal of the Korean Wood Science and Technology 51(5): 321-333.

Kim, J.I., Park, J.Y., Kong, Y.T., Lee, B.H., Kim, H.J., Roh, J.K. 2002. Performance on flame-retardant polyurethane coatings for wood and wood-based materials. Journal of the Korean Wood Science and Technology 30(2): 172-179.

Kim, J.Y., Park, S.Y., Lee, J.H., Choi, I.G., Choi, J.W. 2017. Sequential solvent fractionation of lignin for selective production of monoaromatics by Ru catalyzed ethanolysis. RSC Advances 7(84): 53117-53125.

Kim, K.H., Kim, J.Y., Kim, C.S., Choi, J.W. 2019. Pyrolysis of lignin obtained from cinnamyl alcohol dehydrogenase (CAD) downregulated *Arabidopsis thaliana*. Journal of the Korean Wood Science and Technology 47(4): 442-450.

Kwak, H.W., Shin, M., Yun, H., Lee, K.H. 2016. Preparation of silk sericin/lignin blend beads for the removal of hexavalent chromium ions. International Journal of Molecular Sciences 17(9): 1466.

Lee, H., Kim, S., Park, M.J. 2021a. Specific surface area characteristic analysis of porous carbon prepared from lignin-polyacrylonitrile copolymer by activation conditions. Journal of the Korean Wood Science and Technology 49(4): 299-314.

Lee, I., Oh, W. 2023. Flexural modulus of larch boards laminated by adhesives with reinforcing material. Journal of the Korean Wood Science and Technology 51(1): 14-22.

Lee, J.H., Kim, K., Jin, X., Kim, T.M., Choi, I.G., Choi, J.W. 2021b. Formation of pure nanoparticles with solvent-fractionated lignin polymers and evaluation of their biocompatibility. International Journal of Biological Macromolecules 183: 660-667.

Li, H., Sun, J.T., Wang, C., Liu, S., Yuan, D., Zhou, X., Tan, J., Stubbs, L., He, C. 2017. High modulus, strength, and toughness polyurethane elastomer based on unmodified lignin. ACS Sustainable Chemistry & Engineering 5(9): 7942-7949.

Novo-Uzal, E., Pomar, F., Gómez Ros, L.V., Espiñeira, J.M., Ros Barceló, A. 2012. Evolutionary History of Lignins. In: Lignins: Biosynthesis, Biodegradation and Bioengineering, Ed. by Jouanin, L. and Lapierre, C. Academic Press, Cambridge, MA, USA. pp. 309-350.

Pang, T., Wang, G., Sun, H., Sui, W., Si, C. 2021. Lignin fractionation: Effective strategy to reduce molecule weight dependent heterogeneity for upgraded lignin valorization. Industrial Crops and Products 165: 113442.

Park, S., Kim, J., Choi, J.H., Kim, J.C., Kim, J., Cho, Y., Jung, S., Kwak, H.W., Choi, I.G. 2023. Biodegradation behavior of acetylated lignin added polylactic acid under thermophilic composting conditions. International Journal of Biological Macromolecules 253(Pt 7): 127472.

Park, S.Y., Choi, J.H., Cho, S.M., Choi, J.W., Choi, I.G. 2020. Structural analysis of open-column fractionation of peracetic acid-treated kraft lignin. Journal of the Korean Wood Science and Technology 48(6): 769-779.

Park, S.Y., Kim, J.Y., Youn, H.J., Choi, J.W. 2018. Fractionation of lignin macromolecules by sequential organic solvents systems and their characterization for further valuable applications. International Journal of Biological Macromolecules 106: 793-802.

Ponnuchamy, V., Gordobil, O., Diaz, R.H., Sandak, A., Sandak, J. 2021. Fractionation of lignin using organic solvents: A combined experimental and theoretical study. International Journal of Biological Macromolecules 168: 792-805.

Tekin, K., Hao, N., Karagoz, S., Ragauskas, A.J. 2018. Ethanol: A promising green solvent for the deconstruction of lignocellulose. ChemSusChem 11(20): 3559-3575.

Wang, Y.Y., Wyman, C.E., Cai, C.M., Ragauskas, A.J. 2019. Lignin-based polyurethanes from unmodified kraft lignin fractionated by sequential precipitation. ACS Applied Polymer Materials 1(7): 1672-1679.

Wang, Z., Yang, X., Zhou, Y., Liu, C. 2013. Mechanical and thermal properties of polyurethane films from peroxy-acid wheat straw lignin. BioResources 8(3): 3833-3843.

Watumlawar, E.C., Park, B.D. 2023. Effects of precipitation pH of black liquor on characteristics of precipitated and acetone-fractionated kraft lignin. Journal of the Korean Wood Science and Technology 51(1): 38-48.

Zendrato, H.M., Devi, Y.S., Masruchin, N., Wistara, N.J. 2021. Soda pulping of torch ginger stem: Promising source of nonwood-based cellulose. Journal of the Korean Wood Science and Technology 49(4): 287-298.